DETECTION AND VISUALIZATION OF NARROW LANE REGIONS IN WORK ZONES USING LIDAR-BASED MOBILE MAPPING SYSTEMS

Yi-Ting Cheng [1], Yi-Chun Lin [1], Radhika Ravi [1], Ayman Habib [1, *]

[1] Lyles School of Civil Engineering, Purdue University, West Lafayette, IN, USA - (cheng331, lin934, ravi22, ahabib)@purdue.edu

KEY WORDS: Lane width estimation; LiDAR; Point cloud; Mobile mapping system

ABSTRACT:

Lane width plays a crucial role in road traffic safety. It is especially important in work zones since narrow lane width significantly reduces the roadway capacity and increases the occurrence of traffic accidents. Mobile Mapping Systems (MMS) equipped with laser scanners and cameras are capable of collecting road surface data in a rapid, cost-effective, and safe manner, and thus serves as a feasible tool for automated lane width evaluation. This paper utilizes LiDAR point cloud collected by an MMS to evaluate the lane width in highway work zones. The approach first divides the point cloud into road surface and non-road surface parts. Lane markings are extracted from the road surface point cloud based on intensity. Computing the normal distance between two adjacent lane markings, the lane width is estimated and the areas with narrow lane width are identified and reported. This approach is tested using a LiDAR dataset collected on a highway with a total length of approximately 40.5 miles. A total of 0.8 miles was detected to have narrow lane width and such areas were reported and visualized on the corresponding images captured by the cameras mounted on the MMS. The result demonstrates the capability of the MMS system as an alternative tool for transportation corridor monitoring.

1. INTRODUCTION

Road markings, road pavement, and other characteristics of roads are crucial factors for road safety inspection, traffic accident reduction, and infrastructure monitoring. Such road characteristics are more critical in work zones since the complex array of signs, construction drums, and lane changes would increase the rate of crashes [1]. During any construction project period, lane markings are frequently removed and repainted for lane changes. These temporary lane markings might result in areas with sub-standard lane width. Federal HighWay Administration (FHWA) reported that there were an estimated 96,626 crashes at work zones in 2015, out of which 642 crashes involved at least one fatality [2]. From the HCM 2010 data in Figure 1 [3], it can be inferred that for the same lane width, the lane capacity in work zones is reduced by 900 vehicles per lane per hour as compared to the lane capacity in regular highway segments. Therefore, efficient work zone monitoring and inspection are essential to protect road users and crew within work zones.

Modern MMSs usually carry both laser scanners and optical cameras as well as a direct geo-referencing system. Imagery provides color information while LiDAR point cloud provides 3D information and intensity data. To detect roads/lane markings from imagery, the localization of road borders or lane markings is one of the commonly used approaches [4]. The difficulty of feature extraction from imagery depends on illumination conditions, camera exposure, obstacles, and shadows. Prior work on LiDAR data for road networks focuses on two aspects: 1) using geometric information from LiDAR point cloud to extract road features, and 2) using intensity information from LiDAR data to extract lane markers. Gargoum et al. [5] provided a review of available approaches for the extraction of road features using LiDAR data. They categorized the features into on-road information (road surface, lane markings, and road edge), road side information (traffic signs), road side objects (lamp posts, trees, and utility poles), and geometric information and assessment (road cross section information, vertical alignment information, pavement condition assessment and monitoring, sight distance assessment, and vertical clearance assessment). Guan et al. [6] provided a review of using mobile LiDAR for road information inventory. Three classes of road features – road pavements, road surface structures (road markings, manhole covers, and curvilinear pavement cracks), and pole-like objects – were discussed. With regard to utilizing intensity information from LiDAR data for lane marking extraction, Kumar et al. [7] used a set of range-dependent thresholds to extract lane markings in order to account for the fact that the reflected laser pulse intensities from lane markings might fluctuate strongly according to the incident angles and range between the laser beam firing point and its footprint. Yu et al. [8] proposed a multi-segment threshold to mitigate the effects of intensity variation of point clouds acquired from a Riegl VMX-450 scanner. Guan et al. [9] collected point clouds from a Riegl VMX-450 MMS system and extracted lane markings using multiple thresholds.

For road information extraction, most of the previous work has been mainly focusing on deriving the road surface, road markings, and on road characterization, such as determining the slope, curvature, superelevation, and azimuth, but only Holgado-Barco et al. [10] provided a strategy for lane width estimation – one of the key factors in road safety inspection in work zone areas. Yang et al. [11] mentioned that extracted curbs and road markings can be used to derive road attributes, such as lane width and number of lanes, but there is no proposed strategy or experiment about lane width derivation in the paper. Holgado-Barco et al. [10] proposed a method for extracting road cross-section information. However, their approach is only suitable for 2D laser scanners capturing data at a sufficiently high driving speed as it relies on the separation of individual scan lines and hence, it cannot be extended to other types of laser scanners or dense LiDAR data captured at slower speeds. Moreover, their strategy requires the availability of raw measurements of captured points, such as timestamp and scan angle. They use a scan angle threshold, that is determined for a specific location of the sensors onboard the MMS, for roadway segmentation and

* Corresponding author

hence, it cannot be used for other MMS with different location of laser scanners onboard the vehicle.

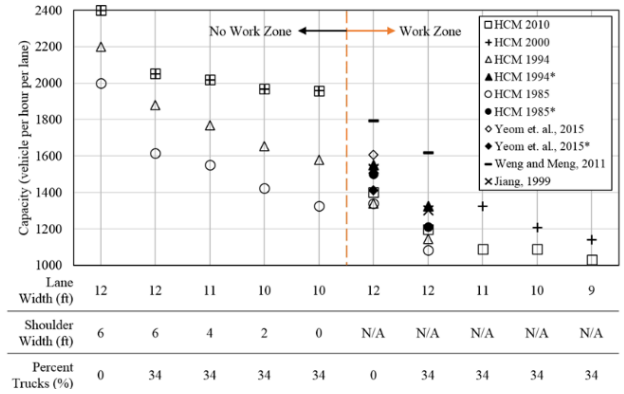

Figure 1. Summary of freeway capacity estimation [3]

2. DATA ACQUISITION SYSTEM

A wheel-based MMS equipped with a Velodyne VLP-16 laser scanner, three Velodyne HDL-32E laser scanners, three Grasshopper cameras (two forward-viewing and one rear-viewing), and an Applanix POSLV 220 GNSS/INS, as shown in Figure 2, is used in this study to acquire data effectively in highway work zones. The onboard Grasshopper cameras are all synchronized to capture images at a rate of 1 frame per second per camera.

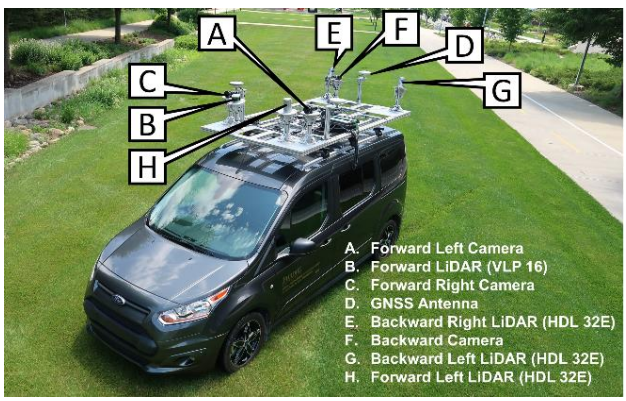

Figure 2. Mobile mapping system used for data acquisition

3. METHODOLOGY

This paper aims to evaluate the lane width in highway work zones and in turn, identify and report regions of interest (ROIs) with narrow lanes. The steps involved in the detection and reporting of narrow lane width areas are depicted using the flowchart in Figure 3. The following subsections introduce the technical details of the six steps shown in the flowchart.

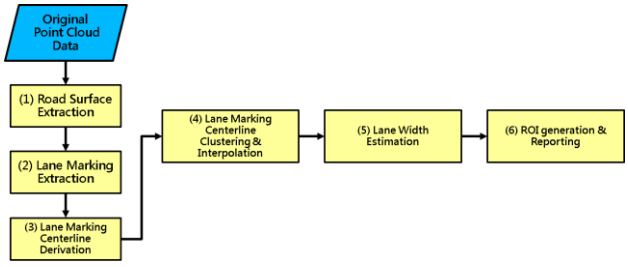

Figure 3. Flowchart of proposed narrow lane width area detection strategy

3.1 Road Surface Extraction

In this step, the vehicle elevation trajectory data and the IMU height above the road surface are utilized to extract the LiDAR point cloud pertaining to the road surface from the original point cloud data. The height threshold (h_{IMU}), as shown in Figure 4, denotes the expected normal distance from the IMU body frame to road surface. The value of h_{IMU} is automatically derived by first, randomly selecting a trajectory elevation data point and searching the LiDAR point (*Pi*) with the closest (X, Y) coordinates and the least Z-coordinate. Then, a k-nearest neighbor search is applied to *Pi* to define a road surface. Finally, the height threshold (h_{IMU}) is derived from the normal distance between the trajectory elevation data point to the fitted plane of the extracted road surface around *Pi*. In addition, a height buffer (h_{buff}) is adopted in this road surface extraction procedure, as shown in Figure 4, since road surface along highways are usually not flat because of a 2% pavement cross slope to ensure proper drainage [12].

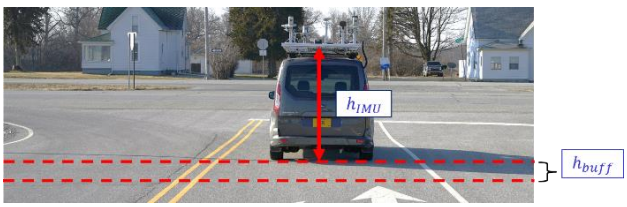

Figure 4. Height threshold (h_{IMU}) and height buffer (h_{buff})

3.2 Lane Marking Extraction

After extracting the road surface, the next step is lane marking extraction that identifies the LiDAR point cloud representing lane markings from the extracted road surface point cloud data. Transportation agencies apply reflective glass beads to lane markings, thus resulting in lane markings appearing as high intensity points in the road surface point cloud. Therefore, the potential lane marking points can be extracted by identifying points belonging to the upper spectrum of intensity distribution of points along the road surface. We starts by constructing a frequency distribution curve of intensity values of the road surface point cloud, as shown in Figure 5. Finally, the road surface points in the top 5th percentile of the intensity frequency distribution are extracted as potential lane marking points, as shown in Figure 6.

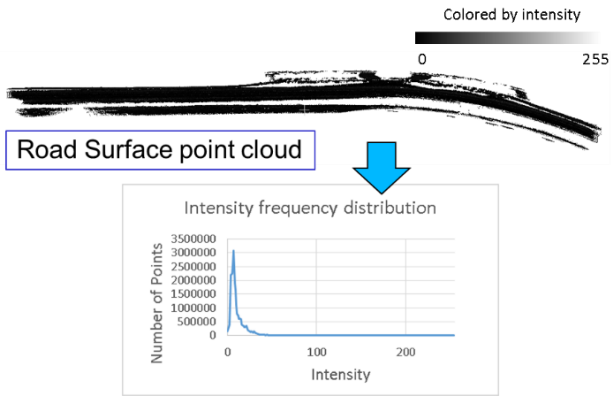

Figure 5. Road surface colored by intensity and the corresponding frequency distribution curve of intensity values

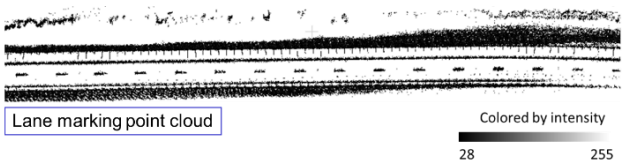

Figure 6. Potential lane markings using the top 5th percentile intensity data

3.3 Lane Marking Centerline Derivation

The potential lane marking points extracted in Section 3.2 may be contaminated by road markings, road surface pavement, and rubble within highway work zones, as shown in Figure 7 (a). Non-lane marking points should be removed before proceeding to lane marking centerline derivation. Therefore, the derivation of lane marking centerline is achieved using the following steps: (1) clustering potential lane marking points using a distance-based region growing, (2) partitioning such clusters into segments, (3) removing non-lane marking points, and (4) generating and down-sampling lane marking centerline points.

First, a distance-based region growing is conducted to cluster neighboring potential lane marking points, as shown in Figure 7 (b). Furthermore, the clusters with numbers of points less than a threshold are removed in this step. Next, considering the curvature of a highway, each lane marking cluster should be divided into small and straight segments to represent curved lane markings by polylines. In this step, each cluster is partitioned into segments based on a fixed length ($Th_{partition}$) along its main direction, as shown in Figure 7 (c). Next, a Random Sample Consensus (RANSAC) strategy and a trajectory-based noise removal strategy are applied to remove the non-lane marking points. RANSAC is an iterative method to estimate a best fitting line model for the straight segment and detect the outlier points within the segment, as shown in Figure 7 (d). For trajectory-based noise removal strategy, an angular threshold (Th_{angle}) is adopted to remove the clusters that are not parallel to the vehicle trajectory, as shown in Figure 7 (e). Finally, after removing the non-lane marking points using the previous steps, all the lane marking points in each segment are projected onto the corresponding fitting line, as shown in Figure 7 (f). Also, considering the efficiency of computation and display, the projected centreline points are down-sampled to retain centerline points at an interval of 20 cm, as shown in Figure 7 (g).

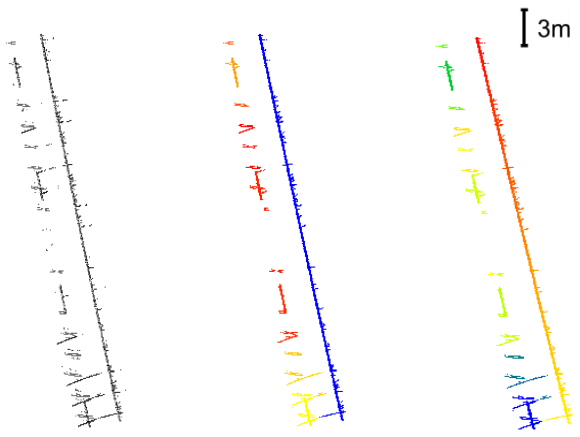

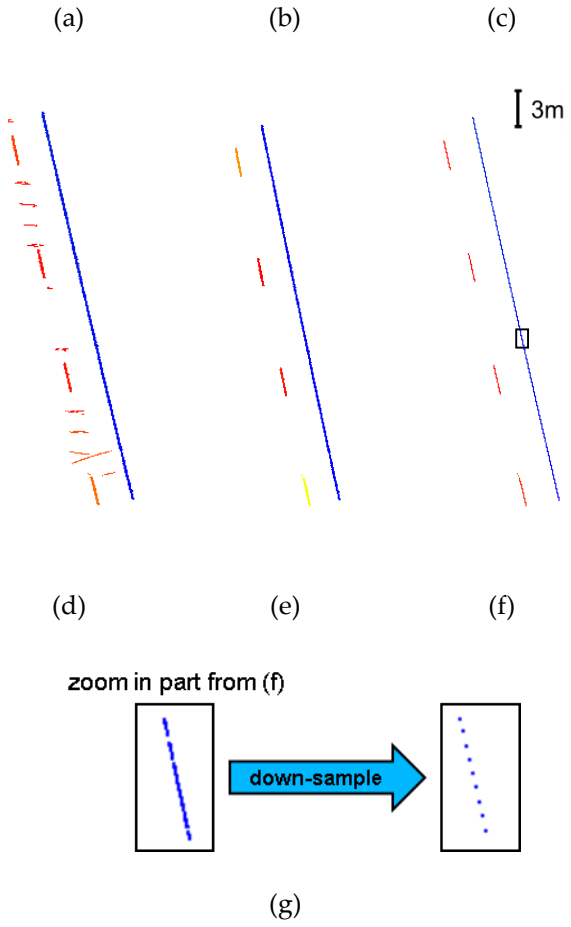

Figure 7. Derivation of lane marking centerline (a) potential lane marking points, (b) distance-based region growing clustering, (c) cluster partition, (d) outlier removal: RANSAC-based, (e) outlier removal: trajectory-based, (f) lane marking centerline, and (g) down-sampled centerline

3.4 Lane Marking Centerline Clustering and Interpolation

This paper aims to estimate the lane width within the driving lane. Therefore, it is imperative to cluster the down-sampled lane marking centerline points derived in Section 3.3 into left and right-hand side (with respect to the driving direction) lane marking groups, as shown in Figure 8.

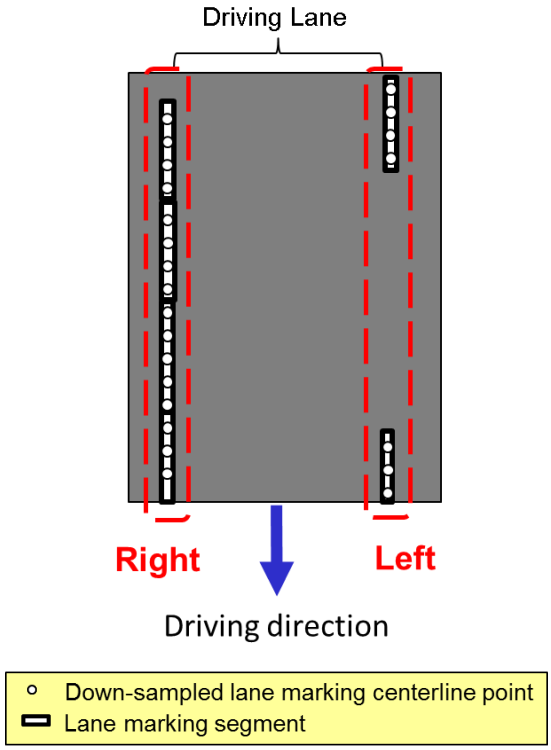

Figure 8. Lane marking centerline clustering

The clustering procedure is achieved first through distance and direction estimation for the down-sampled centerline points. For each query centerline point, we start by defining the original vector joining the query centerline point and its closest trajectory point, denoted as the red vector in Figure 9 (a), and then the projection of this vector perpendicular to the vehicle trajectory is calculated, denoted as the green vector in Figure 9 (a). Next, based on the signed magnitude of the derived projection (denoted as ±d in Figure 9 (a)), the lateral clustering is conducted in order to group together the points with similar lateral distance from the trajectory. Such clusters are marked as initial clusters in Figure 9 (b). Next, a neighboring distance-based region growing (using the distance between down-sampled centerline points) is conducted to group together the laterally separated clusters derived in the previous step that actually belong to the same continuous lane marking, denoted as clusters in Figure 9 (c).

Finally, a linear interpolation is conducted for the derived centerline points if the gap between two successive down-sampled centerline points belonging to the same lane marking cluster (for instance, two centerline points in right lane marking cluster) is larger than 20 cm. This value of 20 cm is same as the down-sampling interval used in Section 3.3. Furthermore, there is no interpolation conducted between two down-sampled centerline points belonging to different lane marking clusters, for instance, one centerline point in right lane marking cluster and another one in left lane marking cluster.

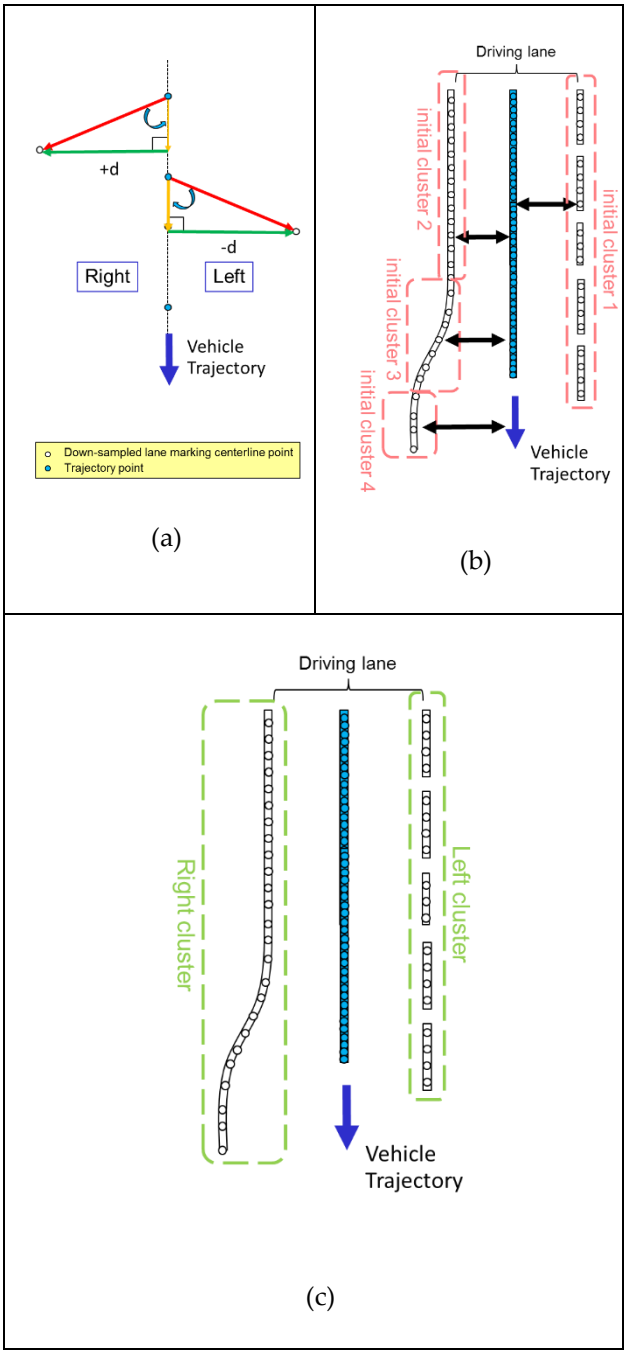

Figure 9. Figurative depiction of lane marking centerline clustering algorithm: (a) distance and direction estimation, (b) lateral distance-based clustering, and (c) neighboring distance-based region growing

3.5 Lane Width Estimation

The lane width along the driving lane is derived as the 3D normal distance between the interpolated centreline points with one belonging to left-hand side lane marking cluster and the other belonging to right-hand side lane marking cluster. First, a 5-nearest neighbor search is applied to the query centerline point (belonging to left-hand side lane marking cluster) to find the neighboring 5 centerline points belonging to right-hand side lane marking cluster, denoted as blue points in Figure 10 (a). Next, the 1st closest centerline point (out of the neighboring 5 centerline points) on the right-hand side that is almost perpendicular to the

driving direction is extracted, as shown in Figure 10 (b). Then, the centerline point closest to the 1st closest centerline point is regarded as the 2nd closest centerline point, as shown in Figure 10 (c). Once the 1st and the 2nd closest centerline points are established, the fitting line of these 2 points can be derived, denoted as a fitting line in Figure 10 (d), and then the query point can be projected onto the fitting line, denoted as a yellow point in Figure 10 (e). Finally, the lane width is estimated by computing the 3D distance between the query point and its corresponding projected point, as shown in Figure 10 (e) and (f). The query point and its corresponding projected point are recorded as a point pair in this procedure. One should note that the standard lane width for Interstate or U.S. Highways is usually 12 ft and it is reduced to 11 ft for work zones. Thus, if a point pair results in a lane width less than 10 ft, then it is recorded as a point pair corresponding to a narrow lane width area.

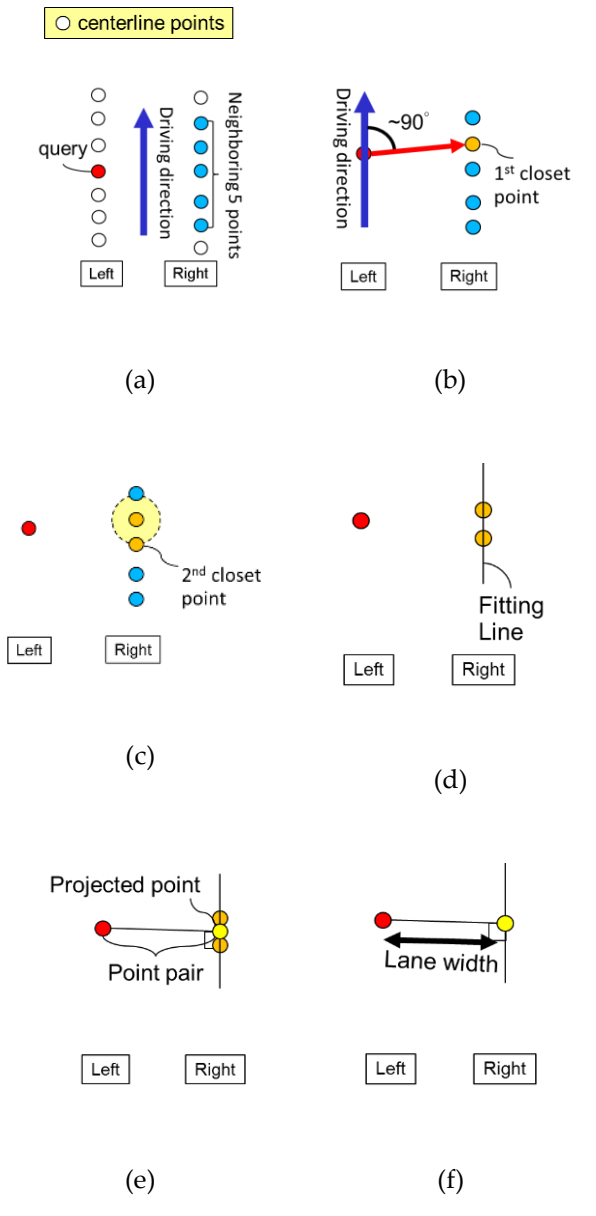

Figure 10. Figurative depiction of lane width estimation algorithm: (a) 5-nearest neighbor search, (b) 1st closest centerline point, (c) 2nd closest centerline point, (d) fitting line, (e) point pair, and (f) lane width

3.6 Region-of-Interest (ROI) Generation and Reporting

In order to report the areas where the lane width is too narrow, this paper proposes an algorithm capable of automatically reporting these areas as regions of interest (ROIs). From section 3.5, the point pairs corresponding to narrow lane width areas are already recorded and these point pairs are used to generate the corresponding ROI. An ROI polygon corresponding to a narrow lane width area is defined by the four points coming from the point pairs marking the start and the end of the region, denoted as a green polygon in Figure 11 (a). Furthermore, to report ROI efficiently, we adjust the reported ROI polygons by merging any two successive ROIs that are less than 10 m apart. This threshold of 10 m is chosen keeping in mind that it is approximately the distance covered in half a second at a speed of 45 miles per hour. Finally, these narrow lane width ROIs are further visualized in two different ways:

1. **3D Visualization:** the ROI polygon is displayed in a red polygon formed by connecting the point pairs marking its beginning and end, as shown in Figure 11 (b) for a sample ROI.
2. **2D Visualization:** The ROI is also visualized for validation using the RGB images captured during the data collection. The image corresponding to the sample ROI is shown in Figure 11 (c).

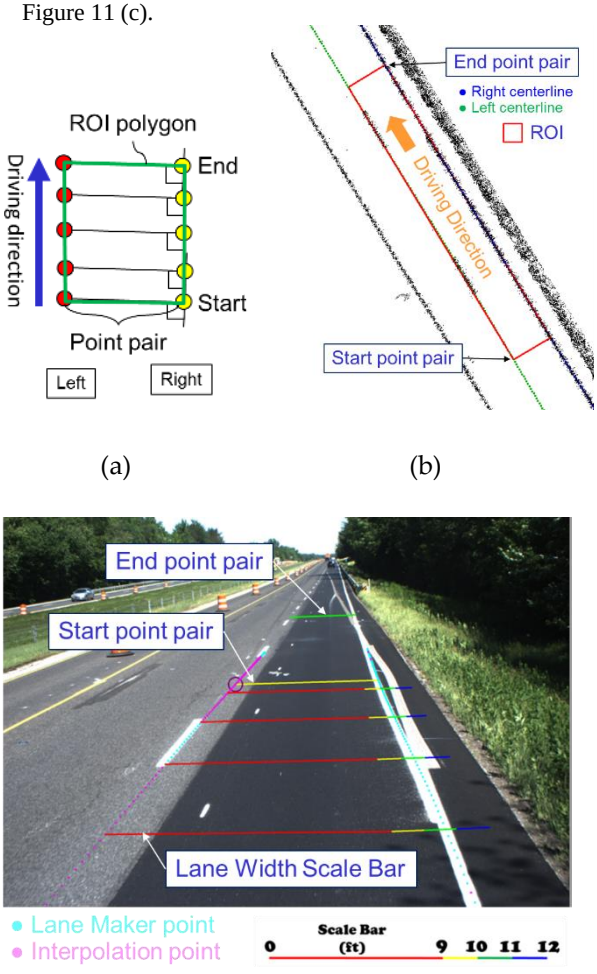

Figure 11. ROI generation and visualization: (a) ROI polygon generation, (b) 3D visualization: ROI polygon overlaid on high intensity lane markings, and (c) 2D visualization: lane marking centerline points and ROI boundary overlaid on RGB imagery

4. RESULTS AND DISCUSSION

4.1 Data Description

This research was conducted in highway work zone areas along 2 Interstate Highways (one South-bound and one West-bound) in the United States, as highlighted in Google Map as shown in Figure 12. These two datasets are surveyed in 2018 to estimate the lane width. The details of these datasets are listed in Table 1.

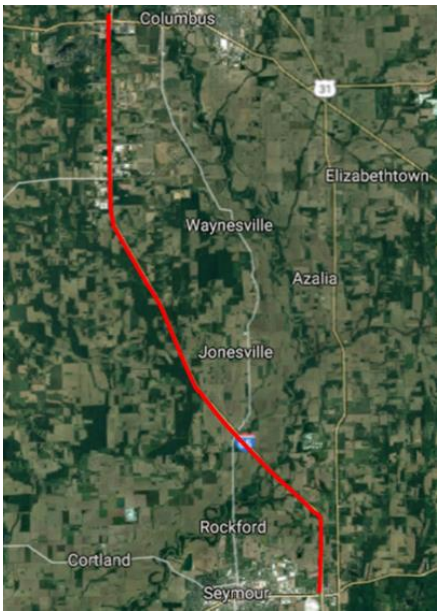

(a)

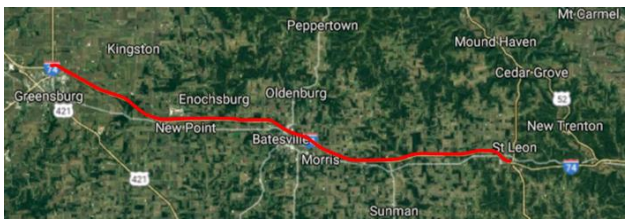

(b)

Figure 12. Location of two datasets and their trajectory (red), (a) Interstate Highway (S), and (b) Interstate Highway (W)

#	Collection Date	Used Sensors	Length	Direction
1	2018/05/24	HDL32E-F HDL32E-L HDL32E-R VLP16	18 miles	South-bound
2	2018/08/09	HDL32E-F HDL32E-L HDL32E-R VLP16	22.5 miles	West-bound

Note: HDL32E-F, HDL32E-L, and HDL32E-R denote different LiDAR sensors of the same model

Table 1. Details of collected datasets in this research

4.2 Lane Width Estimation Results

In the following two sub-sections, two datasets are discussed. Table 2 shows the thresholds used in this paper for these datasets, with a total length of approximately 40.5 miles.

Thresholds	Value
Height buffer for road surface extraction (h_{IMU})	±0.2 m
Minimum number of points of lane marking (Th_{pt})	30 pts
Length of partitioned lane marking segments ($Th_{partition}$)	3 m
Angular threshold for trajectory-based outlier removal (Th_{angle})	20°

Table 2. Thresholds used for lane width estimation

4.2.1 Dataset 1: The estimated lane width values from Mile Post 68 to Mile Post 50 in this southbound road segment along the Interstate highway are shown in Figure 13. There is no narrow lane width ROI in this road segment, as shown in Figure 13.

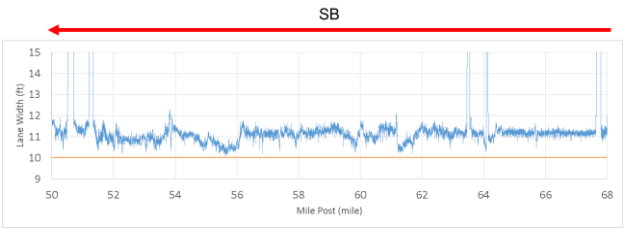

Figure 13. Estimated lane width vs mile post plot for dataset 1

4.2.2 Dataset 2: This westbound road segment from Mile Post 162.5 to Mile Post 140 is divided into three parts, as shown in Figure 14, by a concrete pavement area and a dynamic alignment area for data collection. Figure 15 shows the lane width versus Mile Post data for each part in this road segment. For visual validation, we chose two reported narrow lane ROIs, as highlighted and labeled in the red boxes in Figure 15, in this segment. These ROI visualizations are shown in Figure 16 and Figure 17, respectively. Visual examination of the results in Figure 16 and Figure 17 indicates that narrow lane areas have been correctly reported.

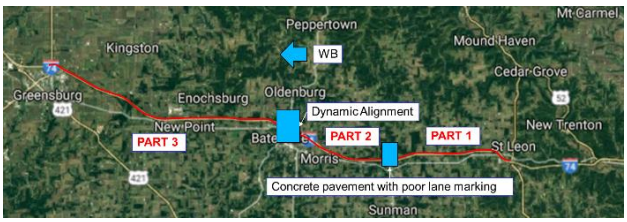

Figure 14. Partition of the Dataset 2 westbound road segment

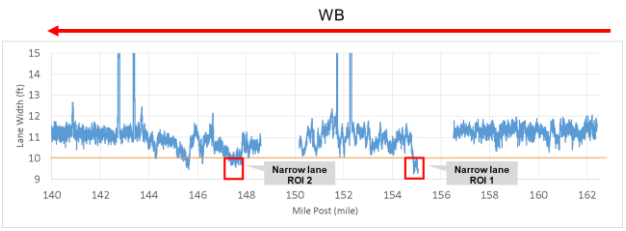

Figure 15. Estimated lane width vs mile post plot for dataset 2

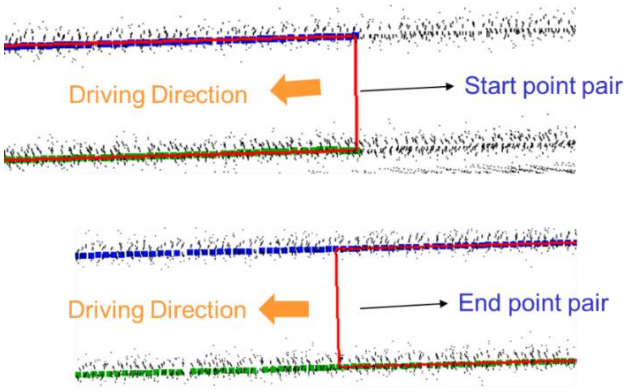

(a)

(b)

Figure 16. Narrow Lane Area 1 in Dataset 2: (a) centerline points and the high intensity map, and (b) corresponding images overlaid with centerline points

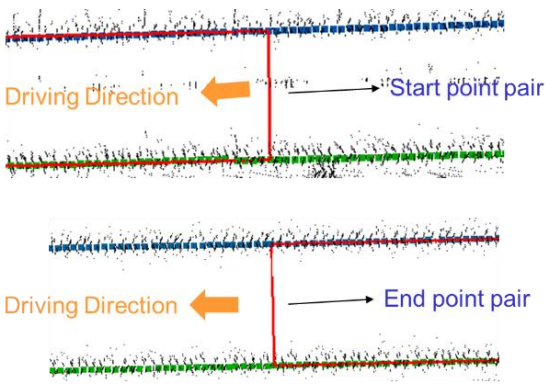

(a)

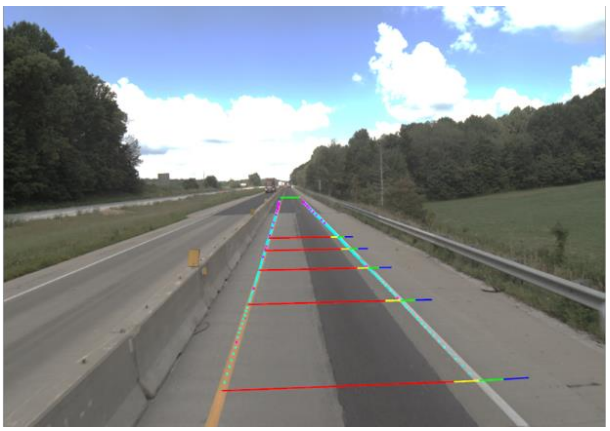

(b)

Figure 17. Narrow Lane Area 2 in Dataset 2: (a) centerline points and the high intensity map, and (b) corresponding images overlaid with centreline points

5. CONCLUSIONS AND RECOMMENDATIONS FOR FUTURE WORK

This paper presents a practical approach for the estimation of lane width using point clouds acquired by a LiDAR-based MMS. The main advantage of the proposed methodology is allowing for the derivation of accurate lane width estimation and reporting of narrow lane width areas while alleviating the risk involved in manual surveying of highway work zones and reducing the incurred cost. In this paper, we used an MMS platform equipped with four laser scanners, three cameras, and GNSS/INS to collect LiDAR point clouds and RGB images along two Interstate Highways in the United States. The experimental results show that the proposed methodology can accurately estimate the lane widths and also, report the ROIs corresponding to areas with narrow lanes (less than 10 ft).

Future research will be focusing on establishing an additional strategy to estimate the lane width not only within the driving lane but also the neighboring lanes. In addition, we aim to exploit other valuable information from LiDAR data in order to detect and report areas with ambiguous lane markings.

ACKNOWLEDGEMENTS

This work was supported in part by the Joint Transportation Research Program administered by the Indiana Department of Transportation and Purdue University. The contents of this paper reflect the views of the authors, who are responsible for the facts and the accuracy of the data presented herein, and do not necessarily reflect the official views or policies of the sponsoring organizations.

REFERENCES

1. Ozturk, O.; Ozbay, K.; Yang, H. Estimating the impact of work zones on highway safety. Transp. Res. Rec. 2014, 14-1873.
2. FHWA Work Zone Facts and Statistics. Available online: https://ops.fhwa.dot.gov/wz/resources/facts_stats/safety.htm (accessed on Oct 18, 2017)
3. Mekker, M. M.; Lin, Y.-J.; Elbahnasawy, M. K. I.; Shamseldin, T. S. A.; Li, H.; Habib, A. F.; Bullock, D. M. Applications of Lidar and Connected Vehicle Data to Evaluate the Impact of Work Zone Geometry on Freeway Traffic Operations. Transp. Res. Rec. (In press)

4. Kong, H.; Audibert, J.-Y.; Ponce, J. General road detection from a single image. *IEEE Trans. Image Process.* **2010**, *19*, 2211–2220.
5. Gargoum, S.; El-Basyouny, K. Automated extraction of road features using LiDAR data: A review of LiDAR applications in transportation. In *Transportation Information and Safety (ICTIS), 2017 4th International Conference on*; IEEE, 2017; pp. 563–574.
6. Guan, H.; Li, J.; Cao, S.; Yu, Y. Use of mobile LiDAR in road information inventory: A review. *Int. J. Image Data Fusion* **2016**, *7*, 219–242.
7. Kumar, P.; McElhinney, C. P.; Lewis, P.; McCarthy, T. Automated road markings extraction from mobile laser scanning data. *Int. J. Appl. Earth Obs. Geoinformation* **2014**, *32*, 125–137.
8. Yu, Y.; Li, J.; Guan, H.; Jia, F.; Wang, C. Learning hierarchical features for automated extraction of road markings from 3-D mobile LiDAR point clouds. *IEEE J. Sel. Top. Appl. Earth Obs. Remote Sens.* **2015**, *8*, 709–726.
9. Guan, H.; Li, J.; Yu, Y.; Wang, C.; Chapman, M.; Yang, B. Using mobile laser scanning data for automated extraction of road markings. *ISPRS J. Photogramm. Remote Sens.* **2014**, *87*, 93–107.
10. Holgado-Barco, A.; Riveiro, B.; González-Aguilera, D.; Arias, P. Automatic inventory of road cross-sections from mobile laser scanning system. *Comput.-Aided Civ. Infrastruct. Eng.* **2017**, *32*, 3–17.
11. Yang, B.; Liu, Y.; Dong, Z.; Liang, F.; Li, B.; Peng, X. 3D local feature BKD to extract road information from mobile laser scanning point clouds. *ISPRS J. Photogramm. Remote Sens.* **2017**, *130*, 329–343.
12. AASHTO, A. Policy on geometric design of highways and streets. Am. Assoc. State Highw. Transp. Off. Wash. DC 2001, 1, 158.